

ORIGINAL ARTICLE

Effect of bioactive glass air-abrasion on *Fusobacterium nucleatum* and *Porphyromonas gingivalis* biofilm formed on moderately rough titanium surface

Faleh Abushahba¹  | Mervi Gürsoy²  | Leena Hupa³  | Timo O. Närhi^{1,4} 

¹Department of Prosthetic Dentistry and Stomatognathic Physiology, Institute of Dentistry, University of Turku, Turku, Finland

²Department of Periodontology, Institute of Dentistry, University of Turku, Turku, Finland

³Johan Gadolin Process Chemistry Centre, Åbo Akademi University, Turku, Finland

⁴Welfare Division, City of Turku, Turku, Finland

Correspondence

Faleh Abushahba, Department of Prosthetic Dentistry and Stomatognathic Physiology, Institute of Dentistry, University of Turku, Lemminkäisenkatu 2, FI-20520, Turku, Finland.
Email: fafabu@utu.fi

Funding information

This study has not received any external funding

Abstract

This aim of this study was to investigate the effects of three types of air-abrasion particles on dual-species biofilms of *Fusobacterium nucleatum* and *Porphyromonas gingivalis*, both of which were cultured on sandblasted and acid-etched (SA) titanium discs. Out of 24 SA discs with biofilm, 18 were exposed to either air-abrasion using Bioglass 45S5 (45S5 BG; $n = 6$), novel zinc (Zn)-containing bioactive glass (Zn4 BG; $n = 6$), or inert glass ($n = 6$). The efficiency of biofilm removal was evaluated using scanning electron microscopy (SEM) imaging and culturing techniques. Air-abrasion using 45S5 BG or Zn4 BG demonstrated a significant decrease in the total number of viable bacteria compared to discs air-abraded with inert glass or intact biofilm without abrasion. Moreover, *P. gingivalis* could not be detected from SEM images nor culture plates after air-abrasion with 45S5 BG or Zn4 BG. The present study showed that air-abrasion with 45S5 or Zn4 bioactive glasses can successfully eradicate dual-biofilm of *F. nucleatum* and *P. gingivalis* from sandblasted and acid-etched titanium discs.

KEYWORDS

air-abrasion, bacteria, bioglass, gram-negative anaerobe, peri-implant infection

INTRODUCTION

Peri-implantitis is defined as a plaque-induced, progressive, and irreversible inflammatory process affecting soft and hard tissues surrounding dental implants [1]. Clinically, it is characterized by redness and swelling in peri-implant mucosa, suppuration, and/or bleeding on probing, along with increased clinical attachment loss and radiographic bone resorption [2,3]. Moreover, based on recent classification and diagnostic criteria, a threshold of ≥ 6 mm pocket depth together with the presence of bleeding and/

or suppuration along with as ≥ 3 mm of marginal bone loss around the implant is the accepted criterion for the diagnosis of peri-implantitis [1,3]. Pathogenic biofilm formation on the implant surfaces due to the inadequate plaque control and irregular maintenance therapy are considered main etiologic factors for the establishment and advancement of peri-implantitis [1,2].

Supra- and subgingival oral microbial biofilms are multilayered and well-structured bacterial communities adhered on the tooth and dental implant surfaces [4–8]. The basic elements of biofilm formation on teeth and dental implant

This is an open access article under the terms of the Creative Commons Attribution License, which permits use, distribution and reproduction in any medium, provided the original work is properly cited.

© 2021 The Authors. *European Journal of Oral Sciences* published by John Wiley & Sons Ltd on behalf of Scandinavian Division of the International Association for Dental Research.

structures are similar and follow an analogous order. First, the protein pellicle adherence on tooth or dental implant surface is required, which is then followed by initial adherence and colonization of predominantly Gram-positive streptococci, anaerobic cocci, and *Actinomyces* species [4]. Multispecies biofilm formation and maturation is enabled by Gram-negative thin rod-shaped *Fusobacterium nucleatum*, as it coaggregates with numerous oral bacterial species and serves as a bridge between primary and secondary colonizers [4,9,10]. The secondary colonizers are typically Gram-negative facultative anaerobic rods (like *Aggregatibacter actinomycetemcomitans*) and strict anaerobes (such as *Porphyromonas gingivalis*, *Treponema denticola*, *Tannerella forsythia*, and *Prevotella intermedia*) [4,9]. The higher occurrence of these periodontal pathogens at peri-implantitis sites than in healthy peri-implant sites and/or teeth with periodontitis has been reported in many studies [7,8,11,12]. Among these pathogens, *P. gingivalis* seems to actively associate with the advancement of peri-implant infection by being more prevalent in the diseased sites [11] and by presenting significantly higher bacterial levels in peri-implantitis [12]. *Porphyromonas gingivalis*' pathogenic role in the disease progression mainly depends on its ability to adhere to host cells and to coaggregate with other bacterial species in the subgingival biofilm [13]. A galactosid moiety on the *P. gingivalis* surface and lectin on *F. nucleatum* surface are used for the coaggregation between the two bacteria [10].

Bacterial biofilm removal from the infected implant surface is considered a crucial component for the management of infection around the dental implant [14,15]. Air-abrasion has been found to be an alternative technique for the removal of biofilm on both natural teeth [16] and dental implants [17]. Air-abrasive devices seem to be efficacious in biofilm removal from both machined and micro-structured implant surfaces without causing roughness or surface changes that can become a bacterial niche [18].

Bioactive glass (BG) is a surface-reactive biomaterial that has antimicrobial and regenerative properties [19,20]. BG antibacterial activity is caused by the elevated pH and osmotic consequences due to the non-physiological concentrations of silicon, calcium, and sodium ions diffused from the glass [19,21]. 45S5 BG has demonstrated a significant antibacterial effect against specific supragingival and subgingival bacteria [21] and it has the potential to decrease the colonization of bacteria and the formation of biofilm [22]. The addition of metal ions to BG has been widely investigated [23–26]. As the glass dissolves, these metal ions are released into the interfacial solution at concentrations that induce the desired antibacterial effect. Zinc (Zn) ions are one of the most potent antibacterial elements that inhibit dental plaque pathogens, including *Streptococcus mutans*, *F. nucleatum*, and *P. gingivalis*

[27–29]. Moreover, the addition of Zn oxide has been found to accelerate bone formation and to enhance BG mechanical properties [30].

Within this background, the current study aimed to test and compare the effects of air-abrasion using 45S5 BG, Zn-containing BG, and inert glass particles on the removal of dual-species biofilm from sandblasted and acid-etched (SA) titanium surface.

MATERIAL AND METHODS

Sandblasting and acid etching of titanium discs

Ti-6Al-4 V ($\alpha + \beta$) titanium alloy square-shaped discs (size 10×10 mm, thickness 1 mm) were first sandblasted on one side with large grit particles of aluminum dioxide (250–500 μm) utilizing 5 bar air pressure at 4 mm distance. Then, the acid etching procedure was performed using a mixture of HCl (60%) and H_2SO_4 (70%) acid at 60°C for 1 h. The titanium discs were then rinsed carefully in deionized water for 20 min utilizing an ultrasonic bath to eliminate acid remnants. The titanium discs were left to dry in a hot air oven at 50°C for 30 min. The SA procedures were performed in-house.

Bioactive glass particle preparation

Zn oxide containing BG (Zn4 BG) and 45S5 BG were prepared in-house. A detailed description of Zn4 and 45S5 BG particle preparation has been explained elsewhere [27]. In short, batches giving 300 g BG were mixed out of analytical grade chemical Na_2CO_3 , $\text{CaHPO}_4 \cdot 2\text{H}_2\text{O}$, ZnO (all from Sigma-Aldrich), CaCO_3 (Fluka), H_3BO_3 (Merck), and Belgian glass quality quartz sand for SiO_2 . The uncovered platinum crucible was used to melt the glasses at 1360°C for 3 h in air. After casting, the resultant glass blocks were annealed at 520°C for 1 h, and then cooled in the oven. The obtained glass blocks were crushed and sieved into the desired fraction (45–120 μm) using stainless steel sieves. No heavy metal contamination induced by the sieves was detected in the glass powder or their immersion solutions.

The glass particle morphology was examined using a scanning electron microscope (SEM; Leo Gemini 1530).

TABLE 1 Nominal composition (mol.%) 45S5 and experimental zinc oxide containing (Zn4) bioactive glasses (BAGs)

	SiO_2	Na_2O	P_2O_5	CaO	ZnO
45S5 BAG	46.1	24.3	2.6	26.9	–
Zn4 BAG	44.1	24.3	2.6	24.9	4.0

The oxide composition of BGs is shown in Table 1. The inert glass in this study was commercial float glass known to be inert in vivo. The glass was crushed and sieved to particles as described above.

Bacterial strains and culture condition

Pure cultures of *F. nucleatum* type strain (ATCC 25586; American Type Culture Collection) and clinical strain of *P. gingivalis* (AHN 24155; the Finnish Institute for Health and Welfare) were transferred from Brucella agar plates to Tryptic Soy Broth (TSB; Sigma Chemical) enriched with hemin (5 mg/L) and menadione (5 mg/L). Bacteria suspensions were cultured in an anaerobic chamber with an atmosphere of 10% H₂, 5% CO₂, and 85% N₂ (Whitley A35 Anaerobic Workstation; Don Whitley Scientific) at 37°C overnight. After incubations, bacterial suspensions were adjusted to the optical density (OD) of 0.5 at 490 nm with a spectrophotometer (Shimadzu Biotech) corresponding to 4×10^7 colony-forming unit (CFU)/ml of *F. nucleatum* and 1.4×10^7 CFU/ml of *P. gingivalis*.

Formation of dual-species biofilm

Prior to the study, the SA discs were disinfected with 70 vol% ethyl alcohol. Afterward, the discs were inserted into 24-well cell culture plates and coated with pasteurized saliva (diluted 1:3 with phosphate buffered saline [PBS]) at 37°C for 30 min. At the end of the coating, the SA discs were rinsed once with PBS and transferred to new wells. Equal amounts (2×10^7 CFU/ml) of *P. gingivalis* and *F. nucleatum* were poured on the discs in fresh culture media and incubated under anaerobic conditions at 37°C for 70 h. After the formation of dual-species biofilms, non-adherent cells were removed by rinsing the discs once with PBS, followed by disc immersion in 2 ml of PBS.

Biofilm removal by air-abrasion with various BG particles

Of the 24 SA discs with the biofilms, 18 were air-abraded with either (a) Zn4 BG ($n = 6$), (b) 45S5 BG ($n = 6$), or (c) inert glass ($n = 6$). The remaining six discs without air-abrasion procedure served as controls (Figure 1). The air-abrasion was performed using an air-polisher device (LM ProPower; LM-Dental) for 20 s, at 90° angles, 3 mm distance, and utilizing 4 bar air pressure. Immediately after air-abrasion, the SA discs were transferred to wells containing 2 ml of fresh TSB (Sigma Chemical) enriched with hemin (5 mg/ml) and menadione (5 mg/ml), and then incubated at 37°C under anaerobic conditions for 23 h.

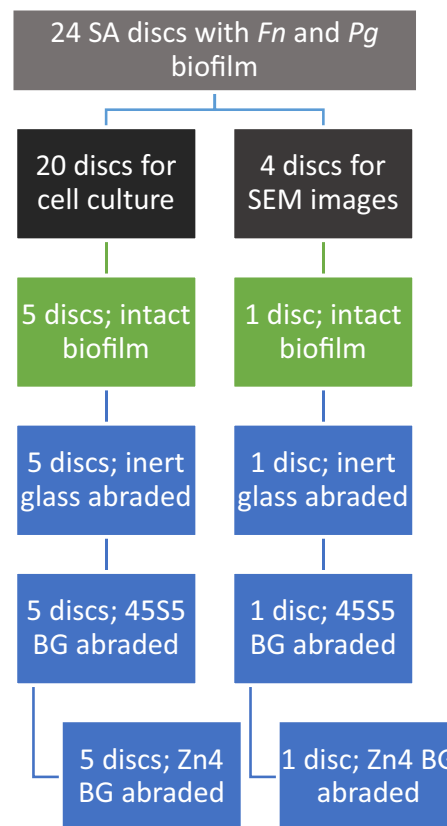


FIGURE 1 Distribution of titanium disc samples exposed to Bioglass 45S5 (45S5 BG), zinc oxide containing BG (Zn4 BG), and inert-glass air-abrasion. The effects of air-abrasion on *Fusobacterium nucleatum* (Fn) and *Porphyromonas gingivalis* (Pg) biofilm formed on sandblasted and acid-etched (SA) titanium surface were confirmed by culture method and scanning electron microscopy (SEM) imaging

Culturing the samples

After incubation, the discs were gently dipped into 10 ml of PBS. Then, the biofilm on each titanium disc was collected with four microbrushes (Quick-Stick; Dentsol). The tips of the brushes used for sampling each disc were placed into a sterile Ebbendorf tube containing 500 µl of TSB (Sigma Chemical) enriched with hemin (5 mg/L) and menadione (5 mg/L). The resulting suspensions were mildly sonicated and serial tenfold dilutions were performed. The diluted bacterial suspensions were cultured on enriched Brucella agar plates and incubated at 37°C for 7 days under anaerobic conditions (Whitley A35 Anaerobic Workstation; Don Whitley Scientific). After incubation, the presence of *F. nucleatum* and *P. gingivalis* on the Brucella agar plates was identified under light microscopy (Leica Microsystems) and they were separated from each other based on their unique colony morphology. The results are expressed as the number of CFUs/SA disc.

Sample preparation for scanning electron microscope

Scanning electron microscopic images were obtained of the surfaces of discs having intact biofilms or having had biofilms removed by air-abrasion with Zn4 BG, 45S5 BG, or particles of inert glass ($n = 4$). Also, SEM images were acquired for discs without biofilm before and after glass air-abrasion ($n = 4$). All discs were washed three times in 1 ml deionized water and then fixed in 2.5% glutaraldehyde overnight at room temperature. Then, the dehydration of the discs was performed by immersion in an ethanol series with gradually increasing concentrations (50%, 70%, 85%, 95%, and 100%) for 10 min each. Five SEM images (Leo 1530; Leo) were obtained at random locations for each disc.

Statistical analyses

For the description of the data, mean values and standard deviations (SDs) were calculated. Statistical analyses were conducted using SPSS (IBM SPSS Statistics for Windows, version 25.0; IBM). One-way ANOVA, followed by Tukey's post hoc, was used to determine the statistical differences between the experimental treatment modalities. The significance level used was 5%.

RESULTS

Statistically significantly lower total bacterial (*F. nucleatum* and *P. gingivalis*) CFUs were observed in dual-species biofilms subjected to BG or inert-glass air-abrasion ($p < 0.001$) than in the intact biofilm (Figure 2). Complete

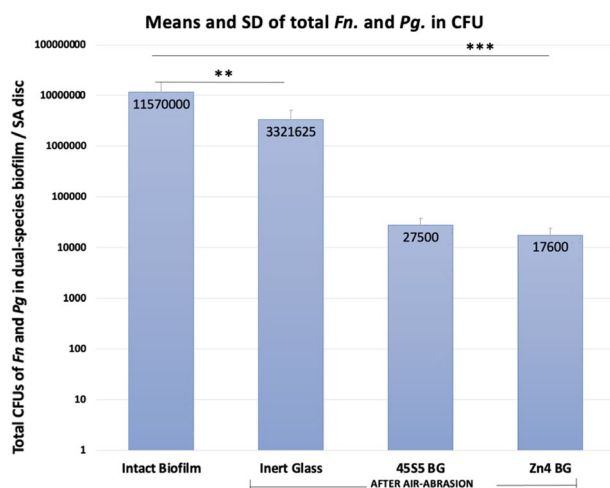


FIGURE 2 Mean colony-forming units (CFUs) \pm SDs of total bacteria *Fusobacterium nucleatum* (Fn) and *Porphyromonas gingivalis* (Pg) on BG/inert-glass air-abraded SA titanium discs. The y-axis is presented in logarithmic scale. Statistical significance, ** $p < 0.05$, *** $p < 0.001$

eradication of *P. gingivalis* was observed following 45S5 and Zn4 air-abrasions in comparison to inert-glass air-abrasion (Figure 3). In addition, air-abrasion using inert glass led to statistically significantly lower *P. gingivalis* CFUs than seen for intact biofilm. The CFUs of *F. nucleatum* were statistically significantly ($p = 0.011$) lower when the biofilm was subjected to BG air-abrasion than when the SA discs were subjected to inert-glass air-abrasion (Figure 4).

The SA disc with intact biofilm showed that the disc was well covered with *F. nucleatum* and *P. gingivalis* after 70 h of incubation (Figure 5A). The SEM images after air-abrasion and further culturing of the samples for 23 h showed no *P. gingivalis* cells on discs air-abraded with 45S5 or Zn4 BGs, whereas these cells were present on discs subjected to inert glass air-abrasion. Fewer *F. nucleatum* cells were observed for 45S5 or Zn4 BGs air-abraded discs than in discs

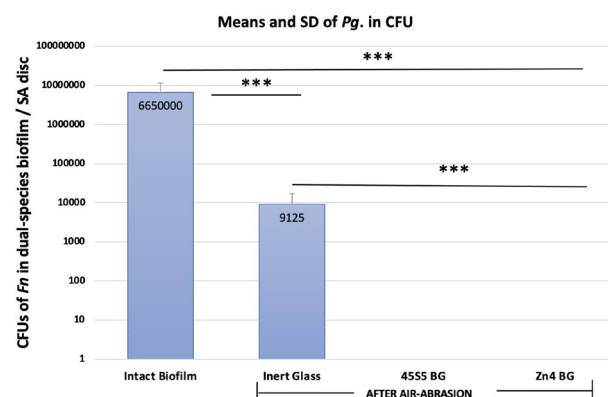


FIGURE 3 Mean colony-forming units (CFUs) \pm SDs of *Porphyromonas gingivalis* (Pg) on BG/inert-glass air-abraded SA titanium discs. The y-axis is presented in logarithmic scale. Statistical significance, *** $p < 0.001$

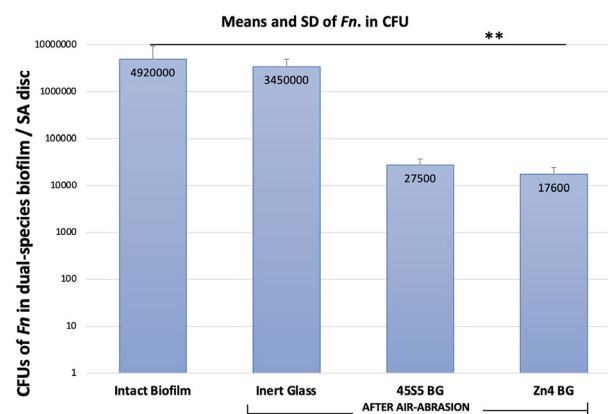


FIGURE 4 Mean colony-forming units (CFUs) \pm SDs of *Fusobacterium nucleatum* (Fn) on BG/inert-glass air-abraded SA titanium discs. The y-axis is presented in logarithmic scale. Statistical significance, ** $p < 0.005$

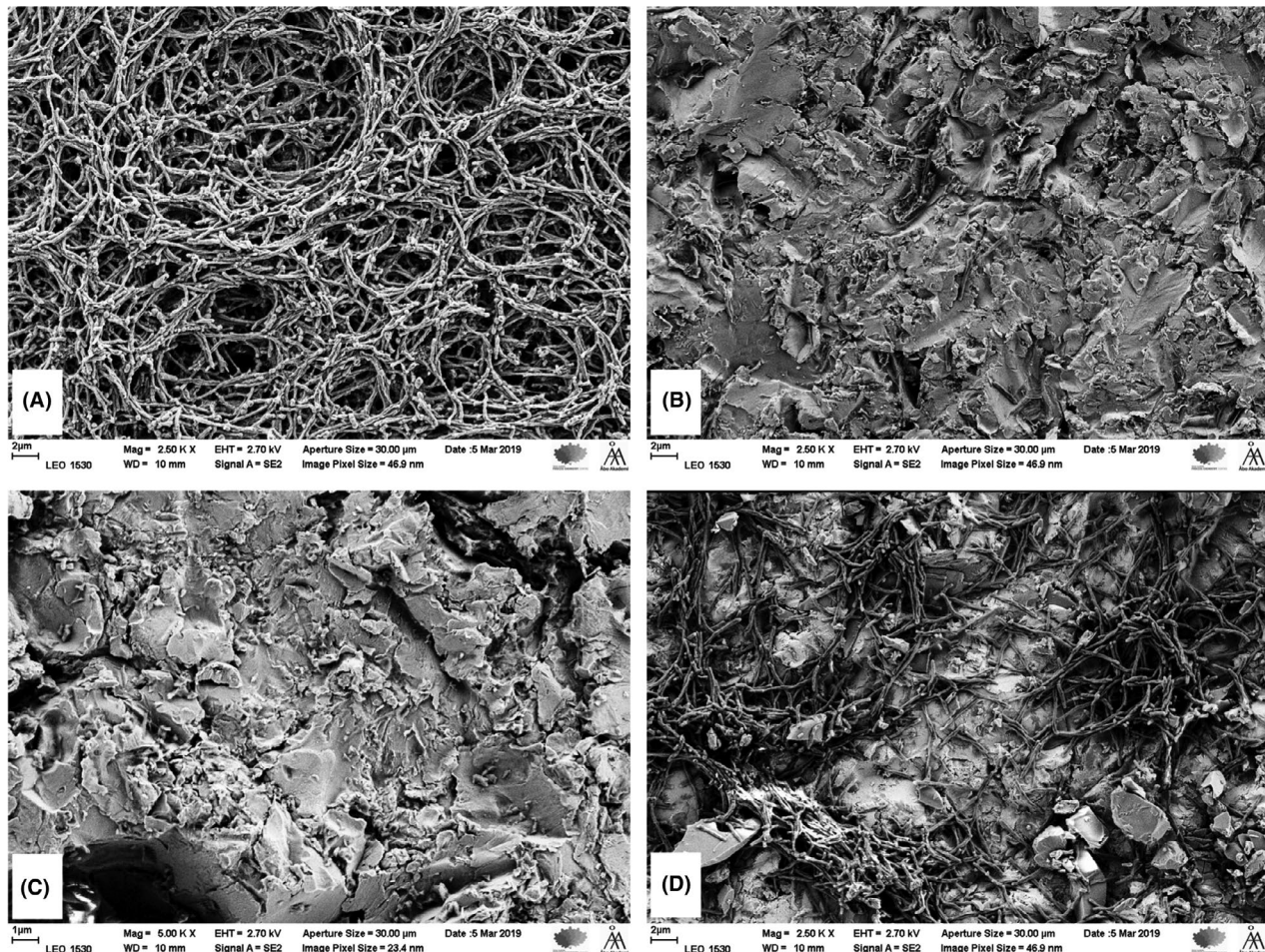


FIGURE 5 Scanning electron microscopy (SEM) images of sandblasted and acid-etched (SA) titanium surfaces along with biofilm at 2.5 KX magnification. Dual-species biofilm of *Fusobacterium nucleatum* and *Porphyromonas gingivalis* prior to air-abrasion (A), and after air-abrasion using 45S5 BG (B), Zn4 BG (C), and inert glass (D)

subjected to inert-glass air-abrasion (Figure 5B–D). Figure 6 shows the SEM images of the SA titanium disc surfaces without biofilm before glass particle air-abrasion (Figure 6A) and after air-abrasion with inert glass, 45S5 BG, and Zn4 BG (Figure 6B–D).

DISCUSSION

The results of this study show that air-abrasion of SA titanium surfaces using either Zn4 BG or 45S5 BG particles completely eradicates *P. gingivalis* and significantly reduced the *F. nucleatum* count from the biofilm, as only *F. nucleatum* cells could be detected on Brucella agars. Air-abrasion with inert glass was also found to be effective in removing *F. nucleatum* and *P. gingivalis* biofilm but was found to be significantly less effective compared to BG particle air-abrasion. This partial outcome is because the effect of the inert glass is limited to mechanical cleaning alone, while both BG formulas evaluated in this study have previously demonstrated

their antimicrobial effects [27]. Additionally, it is possible that the somewhat differing densities of the glasses (45S5 BG – 2.7 g/cm³; Zn4 BG – 2.8 g/cm³; and inert glass – 2.5 g/cm³) may have affected their impact on the surface.

Our previous data [27] have shown that some glass particles remain adhered to or embedded inside the pores on the abraded SA surface after BG air-abrasion. Furthermore, our previous study demonstrated that air-abrasion of SA discs with 45S5 BG, Zn4 BG, or inert glass results in smoother surface topography than is seen for SA without glass particle air-abrasion (Figure 7) [31].

These BG particle residual may explain the extended antibacterial activity of the SA discs [27]. Na⁺, Ca²⁺, and Si ions (dissolved due to BG dissolution) result in an elevation of the pH, which subsequently changes the osmotic pressure of the fluid in the proximity of the BG particles. This is considered the major cause of the antimicrobial effect of BGs against microorganisms [19,21]. A study by ALLAN *et al.* [21] described that exposure of certain bacteria to 45S5 BG, including the bacterial species investigated in this study, resulted

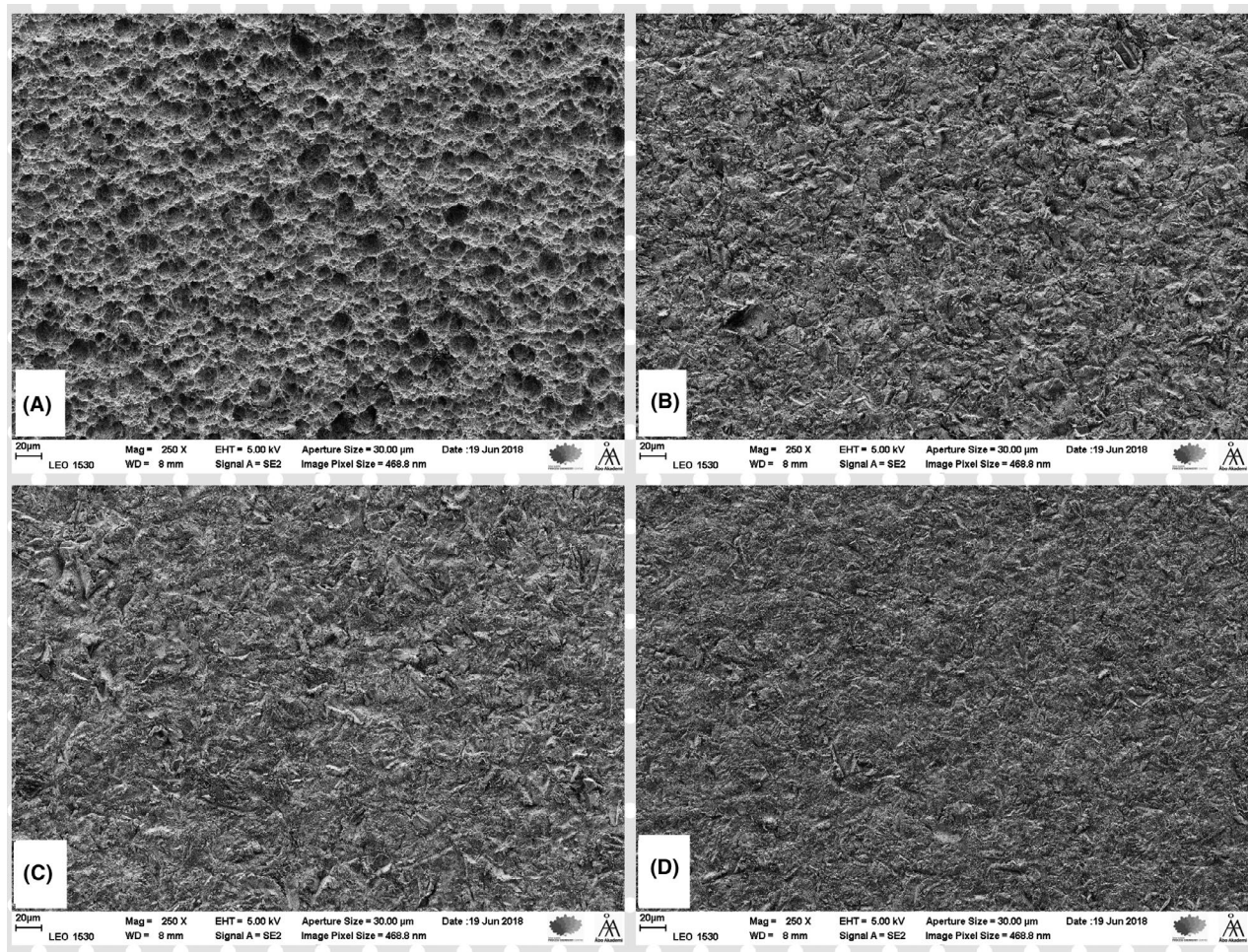


FIGURE 6 Scanning electron microscopy image at 250× magnification of sandblasted and acid-etched titanium surfaces (A), and after air-abrasion with: inert glass (B), 45S5 bioactive glass (C), and Zn4 bioactive glass (D)

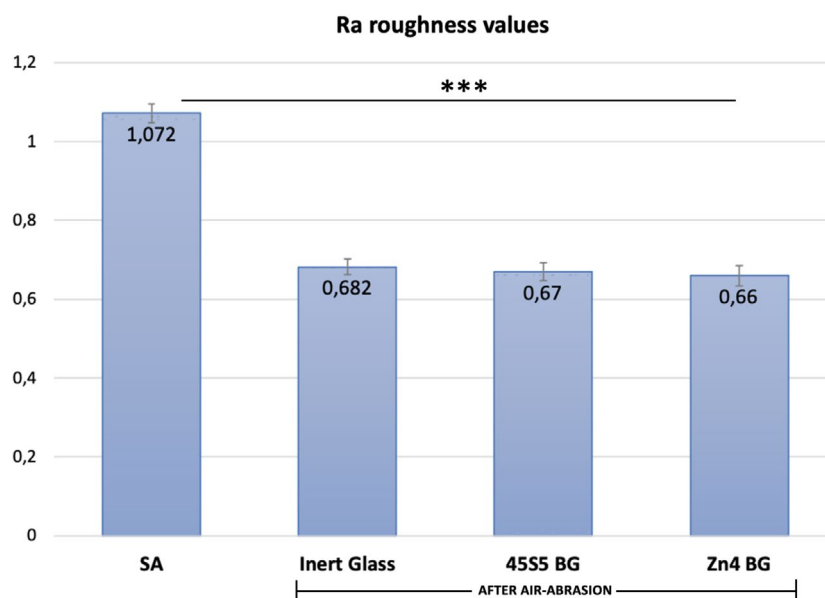


FIGURE 7 Results of surface roughness test performed on sandblasted and acid-etched (SA) titanium discs, and after air-abrasion with inert glass (Inert), 45S5 bioactive glass (45S5 BG), and Zn4 bioactive glass (Zn4 BG). *** $p < 0.001$. Data were extracted from previous publication [31]

in 91.2%–95.0% removal of these bacteria. In their study, they demonstrated that direct contact between the BG particles and bacterial cells is not essential to produce an antibacterial effect.

Our previous study demonstrated that the elevated initial release of Si and Ca^{2+} ions from 45S5 BG resulted in higher pH elevation than Zn4 BG [27]. Therefore, the

mechanism behind the Zn4 BG antibacterial action can not be explained only by the pH elevation [29]. The antibacterial effect of Zn4 may be explained by dissolving Zn^{2+} ions that can penetrate the bacterial cell and produce toxic reactive oxygen species (ROS) that eventually lead to DNA and cell membrane damage [32]. Because of the lower pH elevation, it can be hypothesized that the Zn4 BG is more tissue-friendly than the commercially available 45S5 BG. Additionally, the Zn ion release has been found to stimulate osteoblast cell attachment and proliferation, to inhibit the osteoclastic cells, and to promote in the calcification process [33].

One of the limitations of this study is that the air-abrasion process was conducted in an aerobic environment, which could potentially compromise the viability of *F. nucleatum* and *P. gingivalis*. However, based on our preliminary findings (data not shown), these two microorganisms can survive in the growth media at the aerobic environment for the time needed to perform the air-abrasion process, when they are in their stationary phase. Six samples were taken for air-abrasion at a time, and the process of their air-abrasion lasted for a maximum of 10 min. Moreover, the study was repeated more than two times under similar laboratory conditions. Therefore, the intra-laboratory reproducibility was validated. *Fusobacterium nucleatum* is considered a key micro-organism for the maturation of dental plaque because of its ability to coaggregate and to act as a scaffold between facultative and obligate anaerobic species [9,10]. This is mainly because *F. nucleatum* can survive in an aerobic environment [34]. Indeed, DIAZ *et al.* [35] showed that *F. nucleatum* is able to support the growth of *P. gingivalis* under an oxygenated environment that the latter could not withstand alone. After constructing biofilms, *F. nucleatum* can still increase its numbers, even in aerobic environments [36]. Moreover, recent evidence has revealed that *F. nucleatum* can support the colonization of other anaerobic pathogens by inducing a hypoxia-regulated environmental change [37].

The findings demonstrated in this study are based on dual-species biofilm of *F. nucleatum* and *P. gingivalis* formed in laboratory conditions on SA titanium surfaces. Therefore, the external validity is limited. However, the investigated moderately rough implant surface is widely used in oral implants, and *F. nucleatum* and *P. gingivalis* have been reported to be strongly associated with peri-implantitis [7,8]. Nevertheless, treatment of peri-implantitis using BG air-abrasion needs to be researched in clinical conditions before any conclusion is made.

Within the limitations of this study, it can be concluded that air-abrasion of titanium discs covered with *F. nucleatum* and *P. gingivalis* biofilm utilizing bioactive glass Zn4 and 45S5 particles was effective in the elimination of the biofilm. Hence, their

potential to be used in the decontamination of infected oral implant surfaces needs to be investigated in future in vivo experiments.

ACKNOWLEDGEMENTS

Biomedical research technician Oona Hällfors is kindly acknowledged for her technical assistance in the laboratory.

CONFLICT OF INTERESTS

The authors declare that this paper is original and free of any conflict of interests.

AUTHOR CONTRIBUTIONS

FA contributed to the methodology, investigation, data curation, literature search, writing original draft, and editing the article. **MG** contributed to the methodology, investigation, data curation, writing, editing, and critical review of the article. **LH** contributed to the investigation, writing, editing, and critical review of the article. **TN** contributed to the conceptualization, supervision, reviewing, writing, editing, and critical review of the article. All authors approved the final version of this article.

ORCID

Faleh Abushahba  <https://orcid.org/0000-0002-8032-9396>

Mervi Gürsoy  <https://orcid.org/0000-0001-8545-6821>

Leena Hupa  <https://orcid.org/0000-0001-7745-7779>

Timo O. Närhi  <https://orcid.org/0000-0003-1325-4555>

REFERENCES

1. Berglundh T, Armitage G, Araujo MG, Avila-Ortiz G, Blanco J, Camargo PM, *et al.* Peri-implant diseases and conditions: consensus report of workgroup 4 of the 2017 World workshop on the classification of periodontal and peri-implant diseases and conditions. *J Clin Periodontol.* 2018;45(Suppl 20):S286–91.
2. Schwarz F, Derks J, Monje A, Wang HL. Peri-implantitis. *J Periodontol.* 2018;89(Suppl 1):S267–90.
3. Renvert S, Persson GR, Pirih FQ, Camargo PM. Peri-implant health, peri-implant mucositis, and peri-implantitis: case definitions and diagnostic considerations. *J Clin Periodontol.* 2018;45(Suppl 20):S278–85.
4. Zijngje V, van Leeuwen MB, Degener JE, Abbas F, Thurnheer T, Gmur R, *et al.* Oral biofilm architecture on natural teeth. *PLoS One.* 2010;5:e9321.
5. Furst MM, Salvi GE, Lang NP, Persson GR. Bacterial colonization immediately after installation on oral titanium implants. *Clin Oral Implants Res.* 2007;18:501–8.
6. Mombelli A, Mericske-Stern R. Microbiological features of stable osseointegrated implants used as abutments for overdentures. *Clin Oral Implants Res.* 1990;1:1–7.
7. Sanz M, Newman MG, Nachnani S, Holt R, Stewart R, Flemmig T. Characterization of the subgingival microbial flora around endosteal sapphire dental implants in partially edentulous patients. *Int J Oral Maxillofac Implants.* 1990;5:247–53.
8. Zhuang L, Watt RM, Mattheos N, Si M, Lai H, Lang NP. Periodontal and peri-implant microbiota in patients with healthy

- and inflamed periodontal and peri-implant tissues. Clin Oral Impl Res. 2016;27:13–21.
9. Kolenbrander PE, Palmer RJ Jr, Periasamy S, Jakubovics NS. Oral multispecies biofilm development and the key role of cell-cell distance. Nat Rev Microbiol. 2010;8:471–80.
 10. Kolenbrander PE, Andersen RN, Moore LV. Coaggregation of *Fusobacterium nucleatum*, *Selenomonas flueggei*, *Selenomonas infelix*, *Selenomonas noxia*, and *Selenomonas sputigena* with strains from 11 genera of oral bacteria. Infect Immun. 1989;57:3194–203.
 11. Lafaurie GI, Sabogal MA, Castillo DM, Rincón MV, Gómez LA, Lesmes YA, et al. Microbiome and microbial biofilm profiles of peri-implantitis: a systematic review. J Periodontol. 2017;88:1066–89.
 12. Al-Ahmad A, Muzafferiy F, Anderson AC, Wölber JP, Ratka-Krüger P, Fretwurst T, et al. Shift of microbial composition of peri-implantitis-associated oral biofilm as revealed by 16S rRNA gene cloning. J Med Microbiol. 2018;67:332–40.
 13. How KY, Song KP, Chan KG. *Porphyromonas gingivalis*: an overview of periodontopathic pathogen below the gum line. Front Microbiol. 2016;7:53.
 14. Schwarz F, Mihatovic I, Golubovic V, Bradu S, Sager M, Becker J. Impact of plaque accumulation on the osseointegration of titanium-zirconium alloy and titanium implants. A histological and immunohistochemical analysis. Clin Oral Implants Res. 2015;26:1281–7.
 15. Jepsen S, Berglundh T, Genco R, Aass AM, Demirel K, Derks J, et al. Primary prevention of peri-implantitis: managing peri-implant mucositis. J Clin Periodontol. 2015;42:152–7.
 16. Sculean A, Bastendorf KD, Becker C, Bush B, Einwag J, Lanoway C, et al. A paradigm shift in mechanical biofilm management? subgingival air polishing: a new way to improve mechanical biofilm management in the dental practice. Quintessence Int. 2013;44:475–7.
 17. Tassepe CS, van Waas R, Liu Y, Wismeijer D. Air powder abrasive treatment as an implant surface cleaning method: a literature review. Int J Oral Maxillofac Implants. 2012;27:1461–73.
 18. Louropoulou A, Slot DE, Van der Weijden F. Influence of mechanical instruments on the biocompatibility of titanium dental implants surfaces: a systematic review. Clin Oral Implants Res. 2015;26:841–50.
 19. Stoor P, Söderling E, Salonen JJ. Antibacterial effects of a bioactive glass paste on oral microorganisms. Acta Odontol Scand. 1998;56:161–5.
 20. Jones JR. Review of bioactive glass: from hench to hybrids. Acta Biomater. 2013;9:4457–86.
 21. Allan I, Newman H, Wilson M. Antibacterial activity of particulate bioglass against supra- and subgingival bacteria. Biomaterials. 2001;22:1683–7.
 22. Allan I, Newman H, Wilson M. Particulate bioglass reduces the viability of bacterial biofilms formed on its surface in an in vitro model. Clin Oral Implants Res. 2002;13:53–8.
 23. Du RL, Chang J, Ni SY, Zhai WY, Wang JY. Characterization and in vitro bioactivity of zinc-containing bioactive glass and glass-ceramics. J Biomater Appl. 2006;20:341–60.
 24. Palza H, Escobar B, Bejarano J, Bravo D, Diaz-Dosque M, Perez J. Designing antimicrobial bioactive glass materials with embedded metal ions synthesized by the sol-gel method. Mater Sci Eng C Mater Biol Appl. 2013;33:3795–801.
 25. Hoppe A, Mouriño V, Boccaccini AR. Therapeutic inorganic ions in bioactive glasses to enhance bone formation and beyond. Biomater Sci. 2013;1:254–6.
 26. Goudouri OM, Kontonasaki E, Lohbauer U, Boccaccini AR. Antibacterial properties of metal and metalloid ions in chronic periodontitis and peri-implantitis therapy. Acta Biomater. 2014;10:3795–810.
 27. Abushahba F, Söderling E, Aalto-Setälä L, Sangder J, Hupa L, Närhi T. Antibacterial properties of bioactive glass particle abraded titanium against *Streptococcus mutans*. Biomed Phys Eng Express. 2018;4:045002.
 28. Suzuki N, Nakano Y, Watanabe T, Yoneda M, Hirofujii T, Hanioka T. Two mechanisms of oral malodor inhibition by zinc ions. J Appl Oral Sci. 2018;26:e20170161.
 29. Abushahba F, Söderling E, Aalto-Setälä L, Hupa L, Närhi T. Air abrasion with bioactive glass eradicates *Streptococcus mutans* biofilm from a sandblasted and acid-etched titanium surface. J Oral Implantol. 2019;45:444–50.
 30. Ito A, Kawamura H, Otsuka M, Ikeuchi M, Ohgushi H, Ishikawa K, et al. Zinc-releasing calcium phosphate for stimulating bone formation. Mater Sci Eng C. 2002;22:21–5.
 31. Abushahba F, Tuukkanen J, Aalto-Setälä L, Miinalainen I, Hupa L, Närhi TO. Effect of bioactive glass air-abrasion on the wettability and osteoblast proliferation on sandblasted and acid-etched titanium surfaces. Eur J Oral Sci. 2020;128:160–9.
 32. Yamamoto O. Influence of particle size on the antibacterial activity of zinc oxide. Int J Inorg Mater. 2001;3:643–6.
 33. Ishikawa K, Miyamoto Y, Yuasa T, Ito A, Nagayama M, Suzuki K. Fabrication of Zn containing apatite cement and its initial evaluation using human osteoblastic cells. Biomaterials. 2002;23:423–8.
 34. Diaz PI, Zilm PS, Rogers AH. The response to oxidative stress of *Fusobacterium nucleatum* grown in continuous culture. FEMS Microbiol Lett. 2000;187:31–4.
 35. Diaz PI, Zilm PS, Rogers AH. *Fusobacterium nucleatum* supports the growth of *Porphyromonas gingivalis* in oxygenated and carbon-dioxide-depleted environments. Microbiol. 2002;148:467–72.
 36. Gursoy UK, Pöllänen M, Könönen E, Uitto VJ. Biofilm formation enhances the oxygen tolerance and invasiveness of *Fusobacterium nucleatum* in an oral mucosa culture model. J Periodontol. 2010;81:1084–91.
 37. Mendes RT, Nguyen D, Stephens D, Pamuk F, Fernandes HH, Van TE, et al. Hypoxia-induced endothelial cell responses - possible roles during periodontal disease. Clin Exp Dent Res. 2018;4:241–8.

How to cite this article: Abushahba F, Gürsoy M, Hupa L, Närhi TO. Effect of bioactive glass air-abrasion on *Fusobacterium nucleatum* and *Porphyromonas gingivalis* biofilm formed on moderately rough titanium surface. *Eur J Oral Sci.* 2021;00:e12783. <https://doi.org/10.1111/eos.12783>